

## LETTERS

# A keratin cytoskeletal protein regulates protein synthesis and epithelial cell growth

Seyun Kim<sup>1</sup>, Pauline Wong<sup>1</sup> & Pierre A. Coulombe<sup>1,2</sup>

Cell growth, an increase in mass and size, is a highly regulated cellular event. The Akt/mTOR (mammalian target of rapamycin) signalling pathway has a central role in the control of protein synthesis and thus the growth of cells, tissues and organisms<sup>1</sup>. A striking example of a physiological context requiring rapid cell growth is tissue repair in response to injury<sup>2</sup>. Here we show that keratin 17, an intermediate filament protein rapidly induced in wounded stratified epithelia<sup>3</sup>, regulates cell growth through binding to the adaptor protein 14-3-3 $\sigma$ . Mouse skin keratinocytes lacking keratin 17 (ref. 4) show depressed protein translation and are of smaller size, correlating with decreased Akt/mTOR signalling activity. Other signalling kinases have normal activity, pointing to the specificity of this defect. Two amino acid residues located in the amino-terminal head domain of keratin 17 are required for the serum-dependent relocalization of 14-3-3 $\sigma$  from the nucleus to the cytoplasm, and for the concomitant stimulation of mTOR activity and cell growth. These findings reveal a new and unexpected role for the intermediate filament cytoskeleton in influencing cell growth and size by regulating protein synthesis.

Tissue injury triggers a homeostatic response in which cellular activation, growth and migration are coordinated to achieve repair, defined as the re-establishment of vital functions<sup>2</sup>. The mechanisms responsible for integration of the various aspects of this complex response are unknown. By virtue of their abundance, properties and context-dependent regulation, cytoplasmic intermediate filaments are ideally suited to participate in this integration. These 10–12-nm wide, highly flexible, nonpolar cytoskeletal fibres are formed by a large group of diverse proteins that are differentially distributed and dynamically regulated throughout the body<sup>5</sup>. After injury to skin, wound-proximal epithelial cells increase in size, decrease in adhesiveness and polarize, concomitant with changes in protein regulation and gene expression<sup>2,6</sup>. Among the keratin intermediate filament genes rapidly upregulated in wound-activated skin epithelial cells are *K6* (also known as *Krt6*), *K16* (also known as *Krt16*) and *K17* (also known as *Krt17*) (refs 2, 3). A similar phenomenon, involving distinct intermediate filament genes, occurs in other tissues<sup>7</sup>. Such wound-induced alterations in intermediate filament proteins probably alter cellular viscoelastic properties in a manner that optimizes tissue repair<sup>8</sup>. In light of the large number of signalling proteins already known to interact with intermediate filaments<sup>5,8</sup>, these cytoskeletal fibres are well-placed to fulfill additional, non-mechanical functions during tissue repair and homeostasis.

*K17*-null (*K17*<sup>-/-</sup>) mouse embryos<sup>4</sup> show a delay in the closure of surface ectoderm wounds, but *K6a*<sup>-/-</sup>; *K6b*<sup>-/-</sup> double-knockout embryos do not<sup>9</sup>. To understand this phenotype, we analysed the surface ectoderm in embryonic day (E)11.5 mouse embryos. In wild-type embryos, wound-proximal epithelial cells upregulate *K17*<sup>9</sup> and become significantly enlarged compared to intact tissue (Fig. 1a, b). This hypertrophic response is markedly blunted in *K17*<sup>-/-</sup> embryos (Fig. 1a, b) but not in *K6a*<sup>-/-</sup>; *K6b*<sup>-/-</sup> embryos (data not shown).

Cellular hypertrophy, along with *K6*, *K16* and *K17* upregulation, also occurs in primary cultures of keratinocytes. Cultured *K17*<sup>-/-</sup> keratinocytes are smaller than wild-type controls (Fig. 1c, d). Three-dimensional reconstruction of *K17*<sup>-/-</sup> cells did not reveal changes in cell shape or thickness (data not shown), nor did the absence of *K17* significantly affect cell-matrix adhesion or cell cycling (Supplementary Fig. 1b, c). Thus, we suggest that *K17* may directly affect keratinocyte growth during wound repair and in primary culture.

*De novo* protein synthesis is essential for cell growth. In response to growth factors (Supplementary Fig. 1a), activation of phosphoinositide 3-OH kinase (PI(3)K) and Akt antagonizes the inhibitory

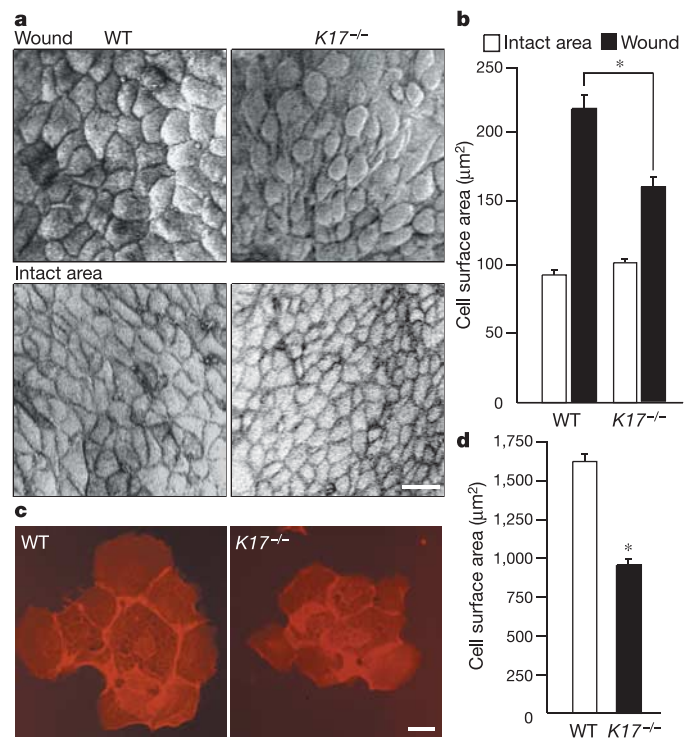


**Figure 1** | *K17*<sup>-/-</sup> keratinocytes are smaller than wild-type cells in the embryonic ectoderm and in primary cultures. **a**, The surface ectoderm of wounded E11.5 mouse embryos was analysed by scanning electron microscopy. Wounded area refers to tissue located within 100 μm of the wound edge, and intact area refers to the upper trunk of embryos. WT, wild type. **b**, Cell surface area measurements performed on preparations shown in **a**. **c**, p120-catenin staining was used to define the outer boundary of cultured keratinocytes<sup>30</sup>. **d**, Cell surface area measurements of cells shown in **c**. For **b** and **d**, *n* > 100 cells for each genotype; data show mean ± s.e.m. Asterisk indicates *P* < 0.01 (Student's *t*-test). Scale bars in **a** and **c**, 20 μm.

<sup>1</sup>Departments of Biological Chemistry and <sup>2</sup>Dermatology, The Johns Hopkins University School of Medicine, Baltimore, Maryland 21205, USA.

activity of the tuberous sclerosis complex (TSC1/TSC2) on mTOR, a serine/threonine kinase with activity important to cell growth<sup>1,10</sup>. TOR-mediated phosphorylation of p70 ribosomal S6 kinase (S6K1) and eukaryotic translation initiation factor 4E-binding protein 1 (4EBP1) stimulates protein synthesis<sup>10,11</sup>. We therefore tested whether lack of K17 alters bulk protein translation and the activity of key regulators. Compared to wild-type cells, cultured *K17*<sup>-/-</sup> keratinocytes have a 15% slower rate of amino acid incorporation into newly synthesized proteins (Fig. 2a), and a 73% slower rate of peptide chain elongation (Fig. 2b). mTOR and Akt activity are also significantly decreased in *K17*<sup>-/-</sup> cells compared to wild-type cells (Fig. 2c and Supplementary Fig. 1d), whereas PI(3)K activity is unaffected (Fig. 2d), suggesting that K17 acts downstream of PI(3)K activation in this pathway (see below). Other kinases, including Erk1/2, p38 MAPK and JNK, have normal activity levels in *K17*<sup>-/-</sup> cells (Fig. 2d), which do not show any signs of cellular stress<sup>12</sup> (Supplementary Fig. 1e). Autophagy is a lysosomal degradation process negatively regulated by mTOR<sup>13</sup>. *K17*<sup>-/-</sup> keratinocytes show increase levels of the processed form of microtubule-associated protein-1 light chain-3 (LC3) (Fig. 2e), an autophagosome marker<sup>14</sup>, as well as the appearance of numerous autophagic vacuoles (Supplementary Fig. 2a). We conclude that the protein synthesis and growth defects in *K17*<sup>-/-</sup> cells are specifically associated with down-regulation of the Akt/mTOR pathway.

We performed additional experiments to characterize *K17*<sup>-/-</sup> keratinocytes. Treatment with rapamycin, a potent mTOR inhibitor<sup>10</sup>, reduces the rate of translation by 22% in wild-type cells and to a lesser extent (7%) in *K17*<sup>-/-</sup> cells, as expected (Supplementary Fig. 1f). Upon serum removal, protein synthesis reaches the same low rate in *K17*<sup>-/-</sup> and wild-type cells (Supplementary Fig. 2b). Serum re-addition causes dramatic stimulation of protein synthesis over 60 min in wild-type keratinocytes. In comparison, the stimulatory

effect of serum on protein synthesis was consistently ~15% lower in *K17*<sup>-/-</sup> keratinocytes (Supplementary Fig. 2b). This depression in translation is also reflected in Akt/mTOR signalling. In wild-type cells, Akt and mTOR are robustly activated upon serum stimulation over at least 150 min. *K17*<sup>-/-</sup> cells show marked activation of Akt 60 min after serum addition, but not at 150 min, and the activity of mTOR remains low in *K17*<sup>-/-</sup> keratinocytes after serum addition (Supplementary Fig. 2b). Although an effect on upstream events cannot be ruled out, these findings imply that loss of K17 primarily affects one or more steps downstream of Akt activation. Given that mTOR can activate Akt<sup>15</sup> (probably as part of a feedback regulatory mechanism), reduced mTOR activation could account for the decreased steady-state activity of Akt in *K17*<sup>-/-</sup> cells (Supplementary Fig. 1a).

To identify K17-binding proteins that might provide mechanistic insight into this growth defect, we set up a biochemical screen using a reversible chemical crosslinker in cultured skin keratinocytes. We identified 14-3-3 $\sigma$  (also known as stratifin), an epithelial-specific isoform of 14-3-3 (ref. 16), as a specific K17-binding protein in keratinocytes (Supplementary Fig. 3a). 14-3-3 proteins regulate many cellular processes by altering the conformation, activity or subcellular localization of target proteins, which they bind in a Ser/Thr-phosphorylation-dependent manner<sup>17,18</sup>. Other intermediate filament proteins also bind 14-3-3 proteins<sup>19,20</sup>; for example, keratin 18 binding influences 14-3-3 distribution and partially

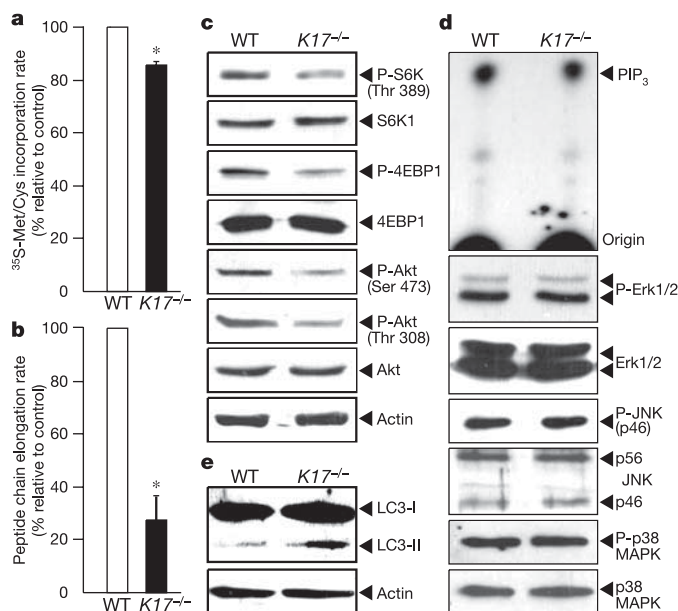


**Figure 2 | Depressed protein translation and Akt/mTOR activity in *K17*<sup>-/-</sup> keratinocytes.** **a**, Total protein synthesis rate was measured by <sup>35</sup>S-methionine/cysteine incorporation into proteins. **b**, Peptide chain elongation rate was determined by measuring the ribosome-transit time<sup>28</sup>. Data in **a**, **b** are mean  $\pm$  s.d.; asterisk indicates  $P < 0.01$  (Student's *t*-test). **c**, Lysates prepared from keratinocytes cultured in growth media were subjected to immunoblot analysis for phosphorylated (P) and non-phosphorylated proteins. **d**, PI(3)K and MAPK activity was assessed by kinase assay and immunoblot analysis, respectively. **e**, Immunoblot analysis for LC3-II, an autophagosome marker. In **c**–**e**, proteins being detected are identified to the right of each blot.

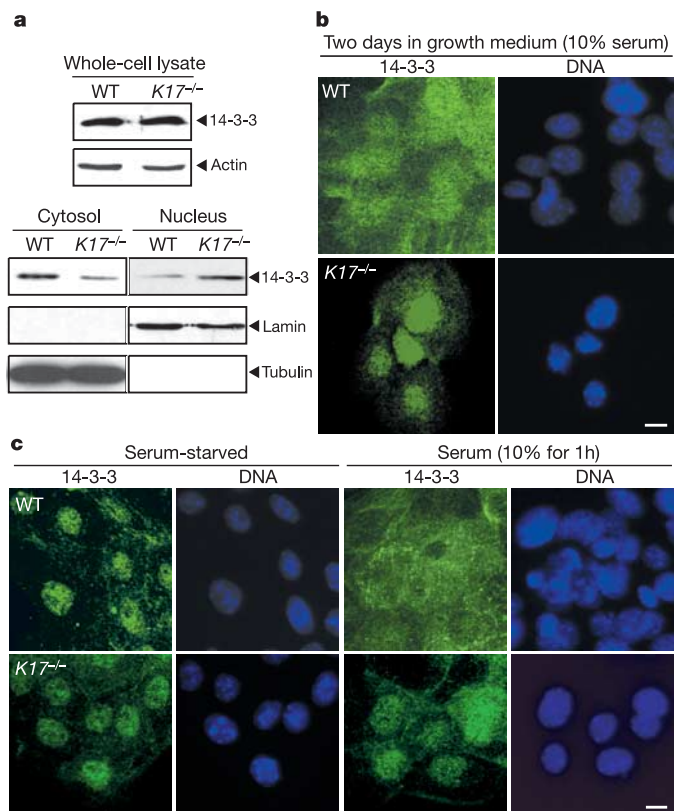


**Figure 3 | Changes in subcellular localization of 14-3-3 proteins in *K17*<sup>-/-</sup> keratinocytes.** **a**, Whole-cell lysates, nuclear fractions and cytosolic fractions were prepared from keratinocytes cultured in growth media and subjected to immunoblot analysis using an anti-total-14-3-3 antibody. Actin is used as a loading control. Tubulin (cytosol) and lamin (nucleus) are used as controls for fractionation and loading. **b**, Immunostaining and confocal microscopy were used to assess the subcellular distribution of 14-3-3 proteins (green) in keratinocytes cultured in growth medium. The vital dye Hoechst was used to identify nuclei (blue). **c**, Cells were serum-starved overnight and then stimulated with 10% FBS for 1 h. 14-3-3 protein localization was determined as in **b**. Scale bars in **b**, **c**, 10  $\mu$ m.

affects mitotic progression in mouse liver hepatocytes<sup>21</sup>. We find that 14-3-3 $\sigma$  colocalizes with K17 in the cytoplasm of skin keratinocytes, where their interaction is phosphorylation-dependent (Supplementary Fig. 3b–d). The distribution of K17 and 14-3-3 $\sigma$  overlaps within hair follicles of intact skin tissue and, notably, in wounded epithelial tissues (Supplementary Fig. 3e). Given this coincidence, along with previous reports proposing 14-3-3 as a positive regulator of the mTOR pathway<sup>22–24</sup> (Supplementary Fig. 1a), we investigated a possible role for 14-3-3 $\sigma$  in the protein synthesis defects seen in  $K17^{-/-}$  cells.

Total 14-3-3 protein levels are similar in wild-type and  $K17^{-/-}$  keratinocytes (Fig. 3a). In wild-type keratinocytes grown in serum-containing growth medium, 14-3-3 $\sigma$  is found in both the cytoplasm and nucleus, but it is found predominantly in the nucleus of  $K17^{-/-}$  cells (Fig. 3a, b). We reasoned that serum, or its physiological equivalent *in vivo*, would probably influence K17 phosphorylation and hence the partitioning of 14-3-3 $\sigma$  in wild-type keratinocytes. Indeed, 14-3-3 proteins redistribute to the nucleus after serum withdrawal in wild-type cultures, and serum treatment causes

them to shift back to the cytoplasm (Fig. 3c). This correlates with increases in K17 phosphorylation and 14-3-3 binding (Supplementary Fig. 3c). In contrast, 14-3-3 remains preferentially localized to the nucleus in serum-stimulated  $K17^{-/-}$  keratinocytes (Fig. 3c), as reported for 14-3-3 mutants unable to bind their partners<sup>18</sup>. Such findings suggest a model (Supplementary Fig. 1a) in which K17 phosphorylation is required for the retention of 14-3-3 in the cytoplasm upon serum stimulation.

Identifying the amino acid residue(s) mediating 14-3-3 binding to K17 should help to define the role of this interaction with regards to protein synthesis. Two consensus 14-3-3-binding sites, threonine 9 (Thr9) and serine 44 (Ser44), are present in the non-helical head domain of K17 (Supplementary Fig. 4a). We mutated these sites to alanine residues and transfected the mutant DNA constructs into BHK fibroblasts. Relative to wild-type K17, T9A and S44A single mutants and the double mutant T9A/S44A show significantly reduced 14-3-3 binding (Supplementary Fig. 4b). The similar loss of binding observed for all mutants implies that Thr9 and Ser44 both contribute to binding to 14-3-3 (ref. 25).

To test for phenotypic rescue, we transiently transfected  $K17^{-/-}$  keratinocytes with wild-type K17, K17(T9A/S44A) or green fluorescent protein (GFP) as a control. Expression of wild-type K17 increases cytoplasmic 14-3-3 levels (Fig. 4a, b) and Akt/mTOR activity (Fig. 4c), increases the rate of protein synthesis by 30% (Fig. 4d) and results in an increased surface area of  $K17^{-/-}$  cells (Fig. 4e). In contrast, although the T9A/S44A mutant becomes readily incorporated into the keratin network, 14-3-3 remains in the nucleus of transfected cells (Fig. 4a, b), and there is no rescue effect on Akt/mTOR activity, translation or cell size (Fig. 4c–e). Moreover, transfection of 14-3-3 $\sigma$ , either alone or together with the T9A/S44A mutant, causes a 20% increase in translation rate in  $K17^{-/-}$  cells, which corroborates the importance of cytosolic 14-3-3 protein levels (Supplementary Fig. 4c). Overexpression of wild-type K17 in wild-type cells has a similar stimulatory effect, but K17(T9A/S44A) overexpression in wild-type cells does not (Supplementary Fig. 4d). We thus suggest that Thr9 and/or Ser44 are required for the physiologically important role of K17 in stimulating Akt/mTOR signalling, protein synthesis and cell growth (Supplementary Fig. 1a).

Given that intermediate filaments are often modulated in wound-activated cells in several tissues<sup>7</sup>, the role we have identified for K17 probably also applies to other family members. In addition to tissue repair, K17 intermediate filaments could modulate keratinocyte growth during skin development and homeostasis as well as in diseases such as psoriasis and carcinoma<sup>26</sup>. These findings add a new dimension to the biological significance of the profound cytoskeletal changes occurring in cells recruited to take part in tissue-remodelling events.

## METHODS

**Mice and cell cultures.**  $K17^{-/-}$  mice were generated as previously described<sup>4</sup>. Skin keratinocytes from newborn mice were isolated and cultured as described<sup>27</sup>. BHK21 fibroblasts were cultured in DMEM medium containing 10% fetal bovine serum (FBS).

**Analysis of cell surface area in embryonic ectoderm and cultured keratinocytes.** Using a Leo FEI scanning electron microscope (Zeiss), we analysed wound-proximal and intact ectoderm from E11.5 embryos that have previously been described<sup>9</sup>. Cell surface area was measured from photomicrographs of the surface ectoderm using MacBAS software. Two-day-old primary cultures of newborn mouse skin keratinocytes were immunostained for p120-catenin to reveal individual cell boundaries, and cell surface area was measured.

**Analysis of cell cycling and plating efficiency.** Relevant methods are described in the legend to Supplementary Fig. 1.

**Rates of total protein synthesis and peptide chain elongation.** Two-day-old primary cultures of newborn mouse skin keratinocytes were labelled with <sup>35</sup>S-methionine/cysteine (0.1 mCi ml<sup>-1</sup>) in methionine- and cysteine-free DMEM for 30 min at 37°C. Proteins were precipitated using trichloroacetic acid (TCA) and the amount of incorporated radioactivity was measured by liquid scintillation. The rate of <sup>35</sup>S-Met/Cys incorporation per min per  $\mu$ g of

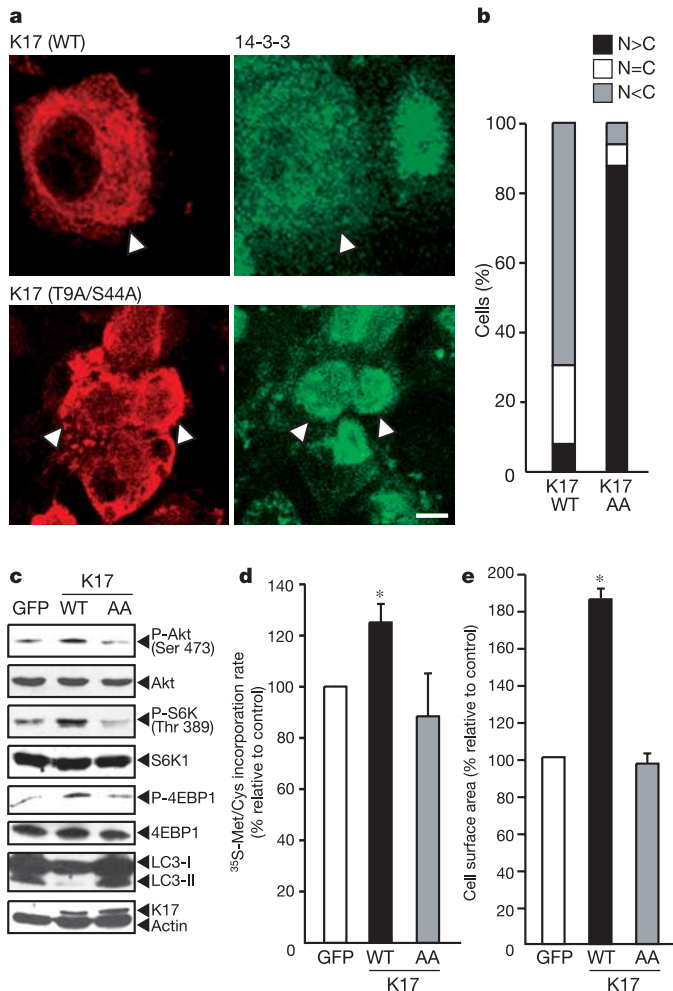


**Figure 4 | Role of K17 in retaining 14-3-3 in the cytoplasm and promoting protein translation and cell growth.** **a**,  $K17^{-/-}$  keratinocytes transfected with wild-type K17 or the K17(T9A/S44A) mutant (AA) were immunostained for K17 (red) and 14-3-3 (green), and analysed by confocal microscopy. Arrowheads point to transfected cells. Scale bar, 10  $\mu$ m. **b**, The 14-3-3 staining pattern was scored for localization to the nucleus (N) or cytoplasm (C) ( $n > 50$  cells in each group). **c–e**, Akt/mTOR activity, translation rate and cell surface area of  $K17^{-/-}$  cells were determined in cells transfected as indicated. Data show mean  $\pm$  s.d. (**d**), mean  $\pm$  s.e.m. (**e**). Asterisk,  $P < 0.01$  (Student's *t*-test). In **e**,  $n > 30$  cells were analysed in each group.

protein was calculated. Translation elongation rate, defined as the inverse of the ribosome transit time, was measured from two-day-old primary cultures of newborn skin keratinocytes from wild-type and *K17<sup>-/-</sup>* mice as previously described<sup>28</sup>.

**Antibodies.** We used antibodies against 14-3-3 $\beta$  (Santa Cruz Biotechnology), 14-3-3 $\sigma$  (from B. Vogelstein), phospho-S473 and phospho-T308 Akt, Akt, phospho-T389 S6K1, S6K1, phospho-Erk, Erk, phospho-p38 MAPK, p38MAPK, phospho-JNK, JNK, phospho-T172 AMPK, AMPK (all from Cell Signalling), Hsp70, Hsp32 (StressGen) and LC3 (from T. Yoshimori).

**<sup>32</sup>P-Metabolic labelling, cell lysis, immunoblotting and immunoprecipitation.** Metabolic labelling was done by incubating cells in phosphate-free DMEM containing 250  $\mu$ Ci ml<sup>-1</sup> <sup>32</sup>P-orthophosphate for 5 h. Lysates were prepared by incubating cells in 20 mM HEPES pH 7.5, 1% NP-40, 120 mM NaCl, 1 mM sodium vanadate, 2 mM NaF, 2.5 mM sodium pyrophosphate, 1 mM EDTA and protease inhibitors. Proteins in the lysates (8–10  $\mu$ g per lane) were resolved by SDS-PAGE and electroblotted. For western blot analysis, bound primary antibodies were detected by enhanced chemiluminescence (Pierce Biotechnology). Immunoprecipitation was also performed from these lysates using anti-K17 antibodies.

**Nuclear and cytosolic fractionation.** Cells were resuspended in hypotonic lysis buffer (20 mM Tris-HCl pH 7.5, 5 mM MgCl<sub>2</sub>, 1 mM sodium vanadate, 10 mM NaF, 1.5 mM KCl, 0.1% NP-40 and protease inhibitors). Cells were incubated on ice for 10 min and homogenized using a 26-gauge syringe. Nuclei were pelleted by centrifugation at 800g for 10 min. The supernatant was centrifuged at 16,000g for 30 min to yield a crude cytoplasmic fraction.

**PI(3)K activity assay.** Cells were lysed in buffer containing 20 mM Tris-HCl pH 7.5, 137 mM NaCl, 1 mM MgCl<sub>2</sub>, 1 mM CaCl<sub>2</sub>, 10% glycerol, 1% NP-40, 150  $\mu$ M sodium vanadate and protease inhibitors. Immunoprecipitates were obtained using anti-phosphotyrosine or anti-PI(3)K p85 subunit antibodies. After washing three times with lysis buffer, twice with 0.5 M LiCl, 100 mM Tris-HCl pH 7.5, and twice with 10 mM Tris-HCl pH 7.4, 100 mM NaCl, 1 mM EDTA, beads were incubated in 50  $\mu$ l kinase buffer (20 mM Tris-HCl pH 7.5, 100 mM NaCl, 0.5 mM EDTA, 70  $\mu$ M phosphoinositide, 40  $\mu$ M ATP, 10  $\mu$ Ci <sup>32</sup>P-ATP) at 22 °C for 20 min. The reaction was stopped by adding 100  $\mu$ l MeOH:HCl (1:1 ratio), and the lipids were extracted with 200  $\mu$ l CHCl<sub>3</sub>:MeOH (1:1 ratio). Phosphorylated lipids were spotted on a thin-layer chromatography (TLC) plate and separated with chloroform:MeOH:ammonium:water at a ratio of 60:47:2:11.3.

**Transfection and cDNA constructs.** For expression in mammalian cells, mouse *K17* cDNA was subcloned into pcDNA3.0 (Invitrogen) harbouring no tag sequence. Mutant *K17* coding sequences, in which alanine residues were introduced at Thr9 (T9A), Ser44 (S44A), and both Thr9 and Ser44, were generated by site-directed mutagenesis (Stratagene). For studies with BHK fibroblasts, *K17* cDNAs were co-transfected with an expression vector encoding mouse *K6a* (ref. 9). Plasmid pHR-14-3-3 $\sigma$ , in which a cytomegalovirus promoter drives human 14-3-3 $\sigma$  expression, was obtained from B. Vogelstein. Transient transfection was performed using Lipofectamine 2000 (Invitrogen).

**Identification of 14-3-3 $\sigma$  as a keratin-17-binding protein.** We modified a protocol making use of a cell-permeable and reversible crosslinker, DSP (dithiobis[succinimidylpropionate])<sup>29</sup>. To increase keratin solubilization, cell lysates were treated with 2% Empigen-BB for 30 min. A 30-kDa band present in *K17* immunoprecipitates was excised, digested with trypsin and analysed by matrix-assisted laser-desorption/ionization time-of-flight (MALDI-TOF) mass spectrometry. Mascot (Matrix Science) was used to identify mouse protein sequences in the NCBI database.

Received 7 December 2005; accepted 17 February 2006.

1. Kozma, S. C. & Thomas, G. Regulation of cell size in growth, development and human disease: PI3K, PKB and S6K. *Bioessays* **24**, 65–71 (2002).
2. Martin, P. Wound healing—aiming for perfect skin regeneration. *Science* **276**, 75–81 (1997).
3. Paladini, R. D., Takahashi, K., Bravo, N. S. & Coulombe, P. A. Onset of re-epithelialization after skin injury correlates with a reorganization of keratin filaments in wound edge keratinocytes: defining a potential role for keratin 16. *J. Cell Biol.* **132**, 381–397 (1996).
4. McGowan, K. M. *et al.* Keratin 17 null mice exhibit age- and strain-dependent alopecia. *Genes Dev.* **16**, 1412–1422 (2002).
5. Omary, M. B., Coulombe, P. A. & McLean, W. H. Intermediate filament proteins and their associated diseases. *N. Engl. J. Med.* **351**, 2087–2100 (2004).

6. Bereiter-Hahn, J. in *Biology of the Integument-Vertebrates* (eds Bereiter-Hahn, J., Matoltsy, A. G. & Richards, K. S.) 443–463 (Springer-Verlag, New York, 1986).
7. DePianto, D. & Coulombe, P. A. Intermediate filaments and tissue repair. *Exp. Cell Res.* **301**, 68–76 (2004).
8. Coulombe, P. A. & Wong, P. Cytoplasmic intermediate filaments revealed as dynamic and multipurpose scaffolds. *Nature Cell Biol.* **6**, 699–706 (2004).
9. Mazzalupo, S., Wong, P., Martin, P. & Coulombe, P. A. Role for keratins 6 and 17 during wound closure in embryonic mouse skin. *Dev. Dyn.* **226**, 356–365 (2003).
10. Hay, N. & Sonenberg, N. Upstream and downstream of mTOR. *Genes Dev.* **18**, 1926–1945 (2004).
11. Fingar, D. C., Salama, S., Tsou, C., Harlow, E. & Blenis, J. Mammalian cell size is controlled by mTOR and its downstream targets S6K1 and 4EBP1/eIF4E. *Genes Dev.* **16**, 1472–1487 (2002).
12. Hardie, D. G. The AMP-activated protein kinase pathway—new players upstream and downstream. *J. Cell Sci.* **117**, 5479–5487 (2004).
13. Meijer, A. J. & Codogno, P. Regulation and role of autophagy in mammalian cells. *Int. J. Biochem. Cell Biol.* **36**, 2445–2462 (2004).
14. Kabeya, Y. *et al.* LC3, a mammalian homologue of yeast Apg8p, is localized in autophagosomal membrane after processing. *EMBO J.* **19**, 5720–5728 (2000).
15. Sarbassov, D. D., Guertin, D. A., Ali, S. M. & Sabatini, D. M. Phosphorylation and regulation of Akt/PKB by the rictor-mTOR complex. *Science* **307**, 1098–1101 (2005).
16. Prasad, G. L., Valverius, E. M., McDuffie, E. & Cooper, H. L. Complementary DNA cloning of a novel epithelial cell marker protein, HME1, that may be down-regulated in neoplastic mammary cells. *Cell Growth Differ.* **3**, 507–513 (1992).
17. Fu, H., Subramanian, R. R. & Masters, S. C. 14-3-3 proteins: structure, function, and regulation. *Annu. Rev. Pharmacol. Toxicol.* **40**, 617–647 (2000).
18. Brunet, A. *et al.* 14-3-3 transits to the nucleus and participates in dynamic nucleocytoplasmic transport. *J. Cell Biol.* **156**, 817–828 (2002).
19. Liao, J. & Omary, M. B. 14-3-3 proteins associate with phosphorylated simple epithelial keratins during cell cycle progression and act as a solubility cofactor. *J. Cell Biol.* **133**, 345–357 (1996).
20. Tzivion, G., Luo, Z. J. & Avruch, J. Calyculin A-induced vimentin phosphorylation sequesters 14-3-3 and displaces other 14-3-3 partners *in vivo*. *J. Biol. Chem.* **275**, 29772–29778 (2000).
21. Ku, N. O., Michie, S., Resurreccion, E. Z., Broome, R. L. & Omary, M. B. Keratin binding to 14-3-3 proteins modulates keratin filaments and hepatocyte mitotic progression. *Proc. Natl Acad. Sci. USA* **99**, 4373–4378 (2002).
22. Beck, T. & Hall, M. N. The TOR signalling pathway controls nuclear localization of nutrient-regulated transcription factors. *Nature* **402**, 689–692 (1999).
23. Bertram, P. G., Zeng, C., Thorson, J., Shaw, A. S. & Zheng, X. F. The 14-3-3 proteins positively regulate rapamycin-sensitive signaling. *Curr. Biol.* **8**, 1259–1267 (1998).
24. Li, Y., Inoki, K., Yeung, R. & Guan, K. L. Regulation of TSC2 by 14-3-3 binding. *J. Biol. Chem.* **277**, 44593–44596 (2002).
25. Yaffe, M. B. *et al.* The structural basis for 14-3-3:phosphopeptide binding specificity. *Cell* **91**, 961–971 (1997).
26. Coulombe, P. A., Tong, X., Mazzalupo, S., Wang, Z. & Wong, P. Great promises yet to be fulfilled: defining keratin intermediate filament function *in vivo*. *Eur. J. Cell Biol.* **83**, 735–746 (2004).
27. Bernot, K. M., Coulombe, P. A. & Wong, P. Skin: an ideal model system to study keratin genes and proteins. *Methods Cell Biol.* **78**, 453–487 (2004).
28. Redpath, N. T., Foulstone, E. J. & Proud, C. G. Regulation of translation elongation factor-2 by insulin via a rapamycin-sensitive signalling pathway. *EMBO J.* **15**, 2291–2297 (1996).
29. Kim, D. H. *et al.* mTOR interacts with raptor to form a nutrient-sensitive complex that signals to the cell growth machinery. *Cell* **110**, 163–175 (2002).
30. Staddon, J. M., Smales, C., Schulze, C., Esch, F. S. & Rubin, L. L. p120, a p120-related protein (p100), and the cadherin/catenin complex. *J. Cell Biol.* **130**, 369–381 (1995).

Supplementary Information is linked to the online version of the paper at [www.nature.com/nature](http://www.nature.com/nature).

**Acknowledgements** We thank members of the Coulombe laboratory for support, B. Vogelstein for providing 14-3-3 $\sigma$  antibody and cDNA, T. Yoshimori for providing anti-LC3 antibody, and C. Parent, S. Craig, J. Lorsch, D. Ginty, S. H. Cha, S. Kim, C. S. Lee and C. Moon for advice. This work was supported by a grant from the National Institute of Arthritis, Musculoskeletal and Skin Diseases (NIAMS) to P.A.C.

**Author Information** Reprints and permissions information is available at [npg.nature.com/reprintsandpermissions](http://npg.nature.com/reprintsandpermissions). The authors declare no competing financial interests. Correspondence and requests for materials should be addressed to P.A.C. ([coulombe@jhmi.edu](mailto:coulombe@jhmi.edu)).